"Multimodal laser ablation/desorption imaging analysis of Zn and MMP-11 in breast tissues"

Raquel González de Vega[1], María Luisa Fernández Sanchez[1], Noemí Eiro[2], Francisco J. Vizoso[2], Michael Sperling[3], Uwe Karst[3] and Alfredo Sanz Medel[1*]

[1] *Department of Physical and Analytical Chemistry, Faculty of Chemistry, University of Oviedo, Spain*

[2] *Research Unit, Hospital de Jove Foundation, Gijón, Spain*

[3] *Institute of Inorganic and Analytical Chemistry, University of Münster, Germany*

*Author to whom correspondence should be addressed

Corresponding authors:

ABSTRACT

Matrix metalloproteinases (MMPs) are a family of zinc-dependent endopeptidases. The main functions of these metalloproteinases are the degradation of the stromal connective tissue and basement membrane components. Recent data from model systems suggest that MMPs are involved in breast cancer (BC) initiation, invasion and metastasis. Particularly, MMP-11 (Stromelysin-3) is expressed in stromal fibroblasts adjacent to epithelial tumor cells, and high levels of this metalloproteinase were associated with tumor progression and poor prognosis of BC. Consequently, MMP-11 involved in these processes can be a candidate as new potential prognostic biomarker in BC.

Bioimaging techniques based on laser ablation/desorption and mass spectrometry are rapidly growing in biology and medicine for studies of biological systems to provide information of biomolecules (such as proteins, metabolites and lipids) and metals with lateral resolution at micrometer scale.

In this study, Matrix-Assisted Laser Desorption/Ionization Mass Spectrometry Imaging (MALDI-MSI) has been used for the first time to investigate the distribution of MMP-11 in human breast cancer tissues in order to show a possible correlation between cancerous and healthy samples, by differential proteomics and using such differences for possible cancer diagnosis and/or prognosis. Additionally, those human breast tissue samples were analyzed in parallel by Laser Ablation-Inductively Coupled Plasma Mass Spectrometry (LA-ICP-MS) in order to gather additional information about the elemental distribution of Zn, and its possible associations with MMPs.

The observed correlation between LA-ICP-MS and MALDI-MSI images warrant further investigations not only to obtain complementary elemental and molecular information about the biomarker MMP-11 but also, by resorting to proper elemental “in-situ” labeling of the protein to using elemental mass spectrometry to develop novel, robust, sensitive and selective, methods for eventual quantifications of very low levels of MMP-11 with ICP-MS detectors.

INTRODUCTION

Breast cancer is one of the leading causes of cancer death among women worldwide. Clinical parameters, such as the size of the primary tumor, the histological grade, classification and regional lymph node involvement, are generally useful for prognosis [1]. The early detection of the disease is vital for a successful patient treatment and supervision. In this sense, the profile of biomarkers may provide valuable insight into the underlying mechanisms of disease progression, thus aiding in understanding the prediction, cause, diagnosis, progression, regression, and outcome of disease treatments [2]. Thus, detection of cancer characteristic biomarkers in tissue sections is essential for the identification and classification of tumor cells and for the choice of the therapy. In the case of breast cancer, estrogen receptor (ER), progesterone receptor (PR) and oncogene Her-2/neu [3, 4] have been investigated as possible biomarkers.

The number of studies on application and better understanding of traditional and new breast cancer biomarkers, and prognostic factors, is continuously growing and they might allow the early identification of individuals with a high risk of breast cancer [5].

During the last years, this type of breast cancer research has been focused on the study of concentration levels of trace elements naturally present in breast tissues, as those levels are considered a promising new tool for cancer prevention, diagnosis and treatment [6]. In this vein, essential elements such as Ca, Fe, Cu and Zn are believed to play key roles, since they are responsible for a great number of metabolic and biological processes. In fact, related to the increased metabolism rates on tumors, trace elements have been shown to appear in altered concentrations in cancer tissues [7]. Therefore, the aforementioned elements concentration levels could be used as potential breast cancer biomarkers.

The role of trace elements in breast cancer is complex, since many types of molecules, cells and tissues are affected [8]. Zinc in particular is a trace element which is vital for numerous cellular processes, particularly the cell growth, playing an important role in cancer etiology and outcome.

Moreover, Zn is a cofactor of the extracellular matrix metalloproteinases (MMPs), a family of 28 zinc-dependent endopeptidases, which are involved in the degradation of the extracellular matrix facilitating the breakdown of the basal membrane and/or matrix connective tissue components [9]. This mechanism is associated with a facilitated proliferation and therefore, the stage of tumor progression is positively correlated with the expression of MMPs in many cases [10]. Particularly, Stromelysine-3 (MMP-11), a matrix metalloproteinase associated with invasion and aggressiveness of cancerous tissue, was postulated as a prognostic marker for pancreatic, breast, and colon cancer patients [11, 12]. Therefore, the combination of epidemiological, analytical and biological studies becomes increasingly relevant for the investigation of the role of Zn and/or MMP-11 in the promotion and/or maintenance of the tumor.

On the other hand, the application of bioimaging techniques based on laser ablation or desorption coupled to MS are rapidly growing in biology and medicine to provide information of key biomolecules (such as proteins, metabolites, and lipids) [13-16] and metals [17- 19] with lateral resolution at the micrometer scale. Such techniques constitute today an important potential tool to study the differential distribution of metals (e.g. Zn) and proteins (e.g. MMP-11) in healthy and cancer breast tissue. Therefore, valuable complementary information regarding the role, uptake, transport, and storage of Zn and MMP-11 and their associations with irregular protein abnormalities can be obtained using a combination of elemental and molecular MS-based imaging techniques.

In this work, two complementary molecular and elemental imaging methods, combining spatially resolved information from Matrix-Assisted Laser Desorption/Ionization-Mass Spectrometry Imaging (MALDI-MSI) and from Laser Ablation-Inductively Coupled Plasma-Mass Spectrometry (LA-ICP-MS), were developed and applied to human breast tissue samples. The observed elemental and molecular spatial distributions are correlated and they are compared with the histological aspects observed for the same breast tissues in an attempt to investigate possible biological implications derived from using such combination of elemental and molecular imaging information.

EXPERIMENTAL

Materials and reagents

All chemicals were used in the highest quality available. Water was purified by an Aquatron water still purification system model A4000D (Barloworld Scientific, Nemours Cedex, France). Rhodium standard solution (1000 mg/L) was purchased from SCP Science (Baie D'Urfé, Canada). Trypsin used for tryptic digestion and α-cyano-4-hydroxycinnamic acid (CHCA) used as matrix were purchased from Sigma-Aldrich (St.Louis, MO, USA). All gases used for ICP-MS and LA analysis (argon and helium, each 99.999% purity) were obtained from Westfalen AG (Münster, Germany).

Tissue sectioning

Frozen breast human tissues samples (healthy and diseased, from the same patients) were provided by the "Biobanco Central de Asturias" (Asturias, Spain) and were stored at -20^{o}C prior to sectioning. Healthy and tumor sections (10-20µm thickness) were prepared using a cryotome (CryoStar NX70, Thermo Scientific, Bremen, Germany) held at -20^{o}C. Tissue slices were thaw-mounted onto glass slides for LA-ICP-MS measurements and for MALDI-MSI measurements, conductive indium-tin oxide (ITO) glass slides (Sigma-Aldrich) were used.

In-situ tryptic digestion

A tryptic digestion was done directly onto the tissue. As a result the identification and distribution of this protein had to be achieved by its peptide fingerprint.

Different tryptic digestion protocols were investigated [20-23], the parameters to be optimized were the following: enzyme concentration (0.05-1 g/L trypsin), solvent (ammonium bicarbonate of different concentration or water), incubation time (2 - 24h), as well as the temperature at which the enzymatic reaction would take place (room temperature or 37ºC). Finally, the following conditions turned out to possess optimal properties: 1 g/L trypsin (Sigma-Aldrich) in bi-distilled water was sprayed three times using an airbrush (Harder & Steenbeck, Germany) (20 psi) onto the tissue and then incubated at 37°C for 24 h. Between the consecutive sprays, the tissue was completely dried.

MALDI Matrix deposition

The MALDI matrix was applied to the digested samples by sublimation onto the sample. In this case, α-cyano-4-hydroxycinnamic acid (CHCA) appeared to have optimal properties to ionize target peptides and was therefore selected in all experiments as matrix. The matrix was applied using an iMLayer (Shimadzu, Kyoto, Japan) (600mg CHCA, 20min, 250^{o}C, 5 x 10^{-2}Pa). This matrix vapor deposition system facilities a controlled matrix deposition with adjusted homogeneous thickness for reproducible sample preparation.

Instrumentation

LA-ICP-MS experiments were carried out using a CETAC LSX-213 laser ablation system (Teledyne CETAC Technologies, Omaha, NE, USA) working at a wavelength of 213nm and hyphenated to an Agilent 7500ce ICP-MS (Agilent Technologies, Santa Clara, USA). Helium was used as carrier gas. The LA-ICP-MS system was tuned for maximum sensitivity prior to each experiment using the reference material NIST 612 "Trace Elements in Glass". The ICP-MS was also tuned to minimize the formation of oxides by monitoring the oxide ratio ($^{232}Th^{16}O^{+}$/ $^{232}Th^{+}$, m/z 248/232) as well as the doubly charge ratio ($^{137}Ba^{++}$/ $^{137}Ba^{+}$, m/z 68.5/137.0). A value of less than 1% for these ratios indicated that the derived signals from potential matrix-based polyatomic interferences were negligible. Furthermore, natural isotopic abundance ratios were monitored to confirm the absence of interfering polyatomic species.

Imaging measurements were performed by multiple line scan ablation of frozen breast tissue sections (line per line) using a spot diameter of 25 µm and no space distance between adjacent lines. A rhodium standard, introduced via liquid sample introduction and merged with the aerosol from the ablation chamber, was used as internal standard in order to compensate plasma fluctuations and surveil plasma stability. Typical operational parameters are summarized in Table 1.

MALDI-MSI experiments were performed using an iMScope TRIO (Shimadzu, Kyoto, Japan), consisting of a mass microscope equipped with an atmospheric pressure ion-source chamber for matrix assisted laser desorption/ionization (AP- MALDI) and a quadrupole ion trap time-of-flight

(QIT-TOF) mass analyzer. The optical microscope combined with the mass spectrometer permitted the precise determination of relevant tissue region prior to performing mass spectrometry imaging (MSI). An ultraviolet laser (355nm) was used to achieve high spatial resolution down to 5µm.

Tissue sections were analyzed in the positive ion mode. The optimized operative conditions of the instrument are listed below and were used for all subsequent measurements of the healthy as well as for the tumor tissue: mass range *m/z*: 600-1600, shots: 100, accumulation: 1, sample voltage: 3.5 kV, detector voltage: 1.90 kV, laser spot size: 25 µm, pixels: (50µm x 50µm). For 2D MSI analysis and overlay of images, data were visualized using "Imaging MS Solution" Software (Shimadzu).

MALDI-MSI data were searched using the MASCOT software against the SwissProt data based and based on the MOWSE algorithm. Within the MASCOT search engine, the enzyme selected was trypsin and experimental ion peptide tolerance was set to ± 1 Da. The criteria also included that one missed cleavage was allowed in order to account for incomplete digestion.

RESULTS AND DISCUSION

Elemental distribution of Zn by LA-ICP-MS

Human breast tissue samples were analyzed by LA-ICP-MS in order to provide information about possible differential spatial distribution of Zn in healthy and tumor samples. Breast samples were prepared as described before and ablated line per line using a focused laser beam. Figure 1 shows the observed Zn distributions of healthy and cancer tissue samples of a selected patient. A rather homogeneous Zn distribution was observed in the healthy tissue (Fig. 1a). In contrast, Fig. 1b shows that Zn distribution in the tumor sample presents hot spots where the amount of Zn is higher than in the rest of the analyzed tissue. Recent work done in our laboratory [24] demonstrated that the level of Zn in breast tumor tissue turned out to be 4 times higher than the corresponding levels found in healthy one (4.7 ± 1.2 µg g^{-1} and 17.8 ± 3.4 µg g^{-1}, respectively). It should be stressed here that increased Zn levels were also found and reported in other studies using X-ray analytical techniques [25, 26]. Although the role of Zn is not yet well clarified in the literature, the observed increased Zn levels in tumor tissues may be associated with structural and metabolic aspects derived from tumor

development. These changes in the Zn levels, associated to cancer, have the potential to provide a novel early biomarker for breast cancer.

Distribution of MMP-11 by means of MALDI-MSI

Using the optimized conditions described in Procedures, the differential protein analysis of healthy and tumor breast tissue samples was carried out by means of MALDI-MSI. Mass spectra from healthy and tumor tissue samples were obtained directly from the in-situ tryptically digested breast tissue sections (see Fig. 2) under study. Fig. 2a shows the obtained spectra of a healthy breast tissue sample. Since a tryptic digestion was performed, protein identification can be carried out through the peptide fingerprint using a data base. A comparatively high number of MMP11-specific peptides was experimentally observed, as compared with those theoretically expected (from the data base) for that protein. Fig. 2b shows the spectra obtained by MALDI-MSI for the tumor tissue (the analysis of tumor sample was conducted under identical conditions). The peptides that belong to the protein of interest (MMP-11) are selected and then introduced in the MASCOT software to assign the found peptide fragments to the target protein.

Comparing the two obtained mass spectra from healthy and tumor samples, it can be seen in Fig. 2 that the tumor sample presents more fragmentation as well as higher signal intensities. This can be due to the higher abundances of the corresponding proteins in the tumor tissue. Table 2 shows the theoretical and the observed masses of the peptides belonging to the digested MMP-11, which were detected in both healthy and tumor tissues (21 and 25 peptides, respectively). These peptides covered the 18% and 20% of the total amino acid sequence of MMP-11 found in healthy and tumor tissue, respectively. As can be seen in the case of tumor tissue (3^{rd} column in Table 2), higher correlations between observed and theoretical peptides (from the data base) were achieved, as well as higher protein sequence coverage. The protein coverage visualizes the mapping of supporting peptides to the target protein.

Two parallel sections (1 and 2) from the tumor tissue were then analyzed and the results were converted into images. The found *m/z* and their respective intensities were measured over the entire

sample and were assigned in a heat map (see Fig. 3). Figure 3a shows the distribution of protonated $[M+H]^+$ ion derived from the proteolytic fragments of MMP-11 at *m/z* 768.5. As can be seen, in both sections, the highly abundant MMP-11 peptides were detected predominantly in one specific area of the tumor sample. Figures 3 b1&b2 correspond to images derived from the overlapping of several MMP-11 peptides at *m/z* 768.5+ 789.6 +822.5 and 735.4+ 744.5 +745.4. As can be seen, all MMP-11 peptides appeared gathering in a specific zone, indicating an increased abundance of this protein in the tumor region. This study shows that the level of MMP-11 was significantly higher in breast cancer tissue than in healthy one. These results are consistent with reports indicating that MMPs are overexpressed in breast cancer and suggesting that the detection of concentrations of MMPs proteins might be useful in distinguishing between benign and malignant breast diseases, as they could be associated with pathologic parameters in breast cancer patients [27]. So MMP-11 might become a potential prognostic marker as well as a therapeutic target for BC patients.

Comparative elemental and molecular results

The observed elevated Zn levels can be associated with an overexpression of the MMP-11(see Fig. 4) but of course, they may be due to other Zn containing enzymes/proteins in the investigated cancer tissue.

In any case, the results from the two complementary (elemental and molecular) imaging techniques tend to confirm that occurrence of Zn and MMP-11 are correlated: this can be observed in Fig. 4, where the distribution of Zn obtained from LA-ICP-MS matched well with the peptide signal obtained by MALDI-MS for the two parallel sections of the analysed breast cancer tissue. In other words, hot spots of Zn occur in the area where maximum intensity of MMP-11 is detected. Thus, complementary imaging information (obtained by elemental and molecular MS techniques of the same samples) has proved useful to correlate Zn levels in the tissue with overexpression of MMP-11, even if the selectivity of measuring MMP-11 via elemental Zn levels by ICP-MS is still debatable.

CONCLUSIONS

In this study, a methodology for the analysis of the potential tumor biomarker MMP-11 in tissue samples was developed (it has been shown that overexpression of this protein is associated with the occurrence of tumor). Initially, different "in-situ" trypsin digestion protocols were applied and optimized (to select the better conditions) to be then applied to in-situ digestion of the MMP-11 protein in healthy and tumor breast tissue samples. It has to be emphasized that the methodology used here of a spraying system for the "in-situ" application of the digestion solution enables to maintain the integrity of the tissue as well as the native distribution of the proteins. The recorded m/z was finally compared with theoretical data for the targeted protein from the data base. By this "in-situ bottom-up" approach, it was possible to assign with spatial resolution the observed specific peptides to their original protein MMP-11. This proceeding is particularly interesting when certain proteins are not easily accessible by conventional MALDI-MSI (e.g., high mass proteins). It was demonstrated that MMP-11 was not homogeneously distributed and showed higher abundances in specific areas of the investigated tissue. Furthermore, higher MMP-11 levels were found in the tumor tissue compared to the healthy one, indicating an altered metabolism and so pointing to MMP-11 as a possible candidate biomarker for breast cancer. Since the protein MMP-11 contains Zn, elemental mapping of the metal by means of LA-ICP-MS was attempted in parallel and images results were compared eventually to those from MALDI-MSI. Images in Fig. 4 show that Zn distribution correlates with the observed abundance of the target protein, MMP-11, indicating that Zn measurement could offer an indirect, more robust and sensitive method for MMP-11 determination [28].

Yet, it should be emphasized that elemental imaging via ICP-MS alone might not be sufficient to trace the MMP-11 distribution, since many different enzymes (and metabolic processes) are reliant upon Zn as cofactor and the required specificity for the Zn-MMP-11 cannot be secured by direct LA-ICP-MS measurements. However, the observed correlation between LA-ICP-MS and MALDI-MSI images in Fig. 4 warrant further investigations in the search for in-situ combined elemental and molecular information of breast cancer tissues. Moreover, by resorting to "in-situ" labeling of MMP-11 (e.g. using bifunctional reagents containing the protein selective antibody bound to metal nanoparticles [29]), extremely sensitive and selective ICP-MS imaging methods can be envisaged for MMP-11.

What is more, absolute quantifications of very low levels of such promising biomarker of breast cancer could be at hand.

ACKNOWLEDMENTS

This work was supported by Projects FC-15-GRUPIN14-092 (Principado de Asturias) and MINECO-13-CTQ2013-49032-C2-1-R (Ministerio de Educación y Ciencia). Parts of this study were supported by the Cells in Motion Cluster of Excellence (CiM-EXC 1003), Münster, Germany (Project FF-2013-17).

REFERENCES

[1] Weigelt, B.; J. L. Peterse; Van ’t Veer, L. J. Breast cancer metastasis: markers and models, *Nat. Rev. Cancer* **2005,** 5, 591-602.

[2] Kang, H. S.; Lee, S. C.; Park, Y. S. *et al*., Protein and lipid MALDI profiles classify breast cancers according to the intrinsic subtype, *BMC Cancer* **2011**, 11, 465-474.

[3]. Kinsella, M. D.; Nassar, A.; Siddiqui M. T.; Cohen, C. Estrogen receptor (ER), progesterone receptor (PR), and HER2 expression pre- and post- neoadjuvant chemotherapy in primary breast carcinoma: a single institutional experience, *Int. J. Clin. Exp. Pathol*. **2012**, 5, 530-536.

[4] Leong, A. S. Y.; Zhuang, Z. The changing role of pathology in breast cancer diagnosis and treatment, *Pathobiology* **2011**, 78, 99-114.

[5] Yersal, O.; Barutca, S. Biological subtypes of breast cancer: Prognostic and therapeutic implications, *World J. Clin. Oncol*. **2014**, 5, 412-424.

[6] Silva, M. P.; Soave, D. F.; Ribeiro-Silva, A.; Poletti, M. E. Trace elements as tumor biomarkers and prognostic factors in breast cancer: a study through energy dispersive x-ray fluorescence, *BMC Res. Note* **2012**, 5, 194-204.

[7] Dang, C. V. Links between metabolism and cancer, *Genes & Dev*. **2012**, 26, 877-890.

[8] Menendez, J. A.; Lupu , R.; *Fatty acid synthase and the lipogenic phenotype in cancer pathogenesis, Nat. Rev. Cancer* **2007**, 7, 763-777.

[9] Meyer, B. S.; Rademann, J.; Extra- and intracellular imaging of human matrix metalloprotease 11 (hMMP-11) with a cell-penetrating FRET substrate, *J. Biol. Chem.* **2012**, 287, 37857-37867.

[10] Figueira, R. C. S.; Gomes, L. R.; Neto, J. S.; Silva, F. C.; Silva, I. D.; Sogaya, M. C. Correlation between MMPs and their inhibitors in breast cancer tumor tissue specimens and in cell lines with different metastatic potential, *BMC Cancer* **2009**, 9, 20-30.

[11] Buache, E.; Thai, R.; Wendling, C.; Alpy, F.; Page, A.; Chenard, M. P.; Dive, V.; Ruff, M.; Dejaegere, A.; Tomasetto, C.; Rio, M. C. Functional relationship between matrix metalloproteinase-11 and matrix metalloproteinase-14, *Cancer Med.* **2014**, 3, 1197-1210.

[12] Pan, W.; Arnone, M.; Kendall, M.; Grafstrom, R. H.; Seitz, S. P.; Wasserman, Z. R.; Albrigh, C. F. Identification of peptide substrates for human MMP-11 (Stromelysin-3) using phage display, *J. Biol. Chem*. **2003**, 278, 27820-27827.

[13] Römpp, A.; Schäfer, K. C.; Guenther, S.; Wang, Z.; Köstler, M.; Leisner, A.; Paschke, C.; Schramm, T.; Spengler, B. High-resolution atmospheric pressure infrared laser desorption/ionization mass spectrometry imaging of biological tissue, *Anal. Bioanal. Chem*. **2013**, 405, 6959-6968.

[14] Wang, H. A. O.; Grolimund, D.; Giesen, C.; Borca, C. N.; Shaw-Stewart, J. R. H.; Bodenmiller, B.; Günther, D. Fast chemical imaging at high spatial resolution by laser ablation inductively coupled plasma mass spectrometry, *Anal. Chem.* **2016**, 85, 10107-10116.

[15] Giesen, C.; Mairinger, T.; Khoury, L.; Waentig, L.; Jakubowski, N.; Panne, U. Multiplexed immunohistochemical detection of tumor markers in breast cancer tissue using laser ablation inductively coupled plasma mass spectrometry, *Anal. Chem.* **2011**, 83, 8177-8183.

[16] Niehoff, A. C.; Kettling, H.; Pirkl, A.; Chiang, Y. N.; Dreisewerd, K.; Yew, J. Y. Analysis of drosophila lipids by matrix-assisted laser desorption/ionization mass spectrometric imaging, *Anal. Chem*. **2014**, 86, 11086-11092.

[17] Becker, J. S.; Matusch, A.; Wu, B. Bioimaging mass spectrometry of trace elements - recent advance and applications of LA-ICP-MS: A review, *Anal. Chim. Acta* **2014**, 835, 1-18.

[18] Konz, I.; Fernández, B.; Fernández, M. L.; Pereiro, R.; González-Iglesias, H.; Coca-Prados, M.; Sanz-Medel, A. Quantitative bioimaging of trace elements in the human lens by LA-ICP-MS, *Anal. Bioanal. Chem*. **2014**, 406, 2343-2348.

[19] Bishop, D. P.; Clases, D.; Fryer, F.; Williams, E.; Wilkins, S.; Hare, D.J.; Cole, N.; Karst, U.; Doble, P. A. Elemental bio-imaging using laser ablation-triple quadrupole-ICP-MS, *J. Anal. At. Spectrom.* **2016**, 31, 197-202.

[20] Groseclose, M. R.; Andersson, M.; Hardesty, W. M.; Caprioli, R. M. Identification of proteins directly from tissue: in situ tryptic digestions coupled with imaging mass spectrometry, *J. Mass Spectrom.* **2007**, 42, 254-262.

[21] Blaze, M. T. M.; Aydin, B.; Carlson, R.; Hanley, L. Identification and imaging of peptides and proteins on enterococcus faecalis biofilms by matrix assisted laser desorption ionization mass spectrometry, *Analyst* **2012**, 137, 5018-5025.

[22] Harris, G. A.; Nicklay, J. J.; Caprioli, R. M. Localized in Situ Hydrogel-Mediated Protein Digestion and Extraction Technique for on-Tissue Analysis, *Anal. Chem.* 2013, 85, 2717-2723.

[23] Stauber, J.; MacAleese, L.; Franck, J.; Claude, E.; Snel, M.; Kaletas, B. K.; Wiel, I. M.; Wisztorski, M.; Fournier, I.; Heeren, R. M. On-tissue protein identification and imaging by MALDI-ion mobility mass spectrometry, *J. Am. Soc. Mass Spectrom*. **2010**, 21, 338-347.

[24] González de Vega, R.; Fernández Sanchez, M. L.; Pisonero, J.; Eiró, N.; Vizoso, F. J.; Sanz Medel, A. Quantitative bioimaging of Ca, Fe, Cu and Zn in breast cancer tissues by LA-ICP-MS, *J. Anal. Atomic Spectrom.* **2016**, DOI: 10.1039/c6ja00390g.

[25] Silva, M. P.; Soave, D. F.; Ribeiro-Silva, A.; Poletti, M. E. Trace elements as tumor biomarkers and prognostic factors in breast cancer: a study through energy dispersive x-ray fluorescence, *BMC Res. Notes* **2012**, 5, 194-204.

[26] Mulware, S. J.; Comparative Trace Elemental Analysis in Cancerous and Noncancerous Human Tissues Using PIXE, *J. Biophysics* **2013** Article ID 192026.

[27] Cid, S.; Eiro, N.; González, L. O.; Beridze, N.; Vazquez, J.; Vizoso, F. J. Expression and clinical significance of metalloproteases and their inhibitors by endothelial cells from invasive breast carcinomas, *Clin. Breast Cancer* **2016**, 16, e83-e91.

[28] Sanz-Medel, A.; "Heteroatom-tagged" quantification of proteins via ICP-MS, *Anal. Bioanal. Chem.* **2016**, 408, 5393-5395.

[29] Garcia-Cortes, M.; Encinar, J.R.; Costa-Fernandez, J.M.; Sanz-Medel, A. Highly sensitive nanoparticle-based immunoassays with elemental detection: Application to Prostate-Specific Antigen quantification, *Biosensors and Bioelectronics* **2016**, 85, 128-134.

LEYEND OF FIGURES

Figure 1 Distribution of Zn in a frozen breast tumor tissue by LA-ICP-MS (a) healthy (b) tumor tissue.

Figure 2 Mass Spectra obtained by MALDI-MSI from a healthy (a) and breast cancer tissue (b) *m/z* range: 600-1000

Figure 3 MALDI Images generated from the found characteristic peptides of the MMP-11, a) A specific peptide signal belongs to MMP-11, *m/z* 768.5; b) Overlay signals of several peptides from MMP-11, *m/z* 768.5+ 789.6 +822.5 and 735.4+ 744.5 +745.4

Figure 4 Comparative images obtained from a frozen breast tumor tissue by LA-ICP-MS and MALDI-MSI techniques

Figure 1

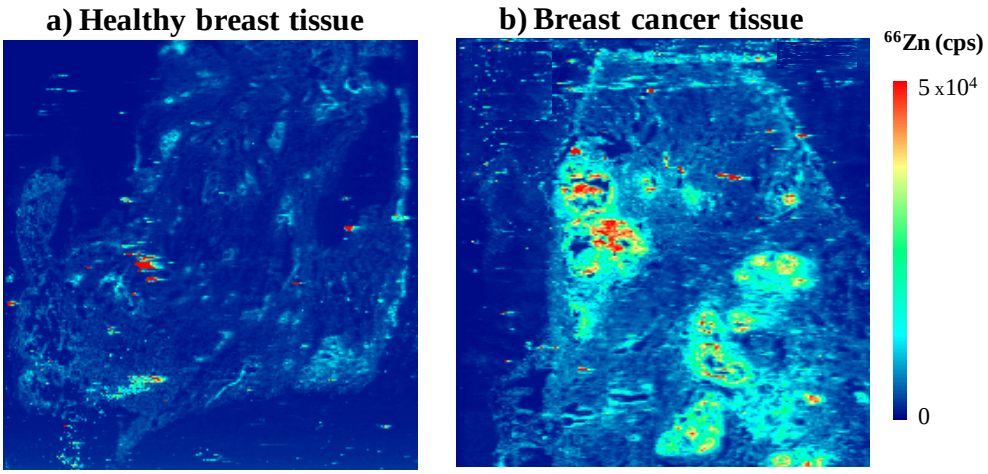
a) Healthy breast tissue
b) Breast cancer tissue
66Zn (cps)
5 x10^4
0

Figure 2

a)

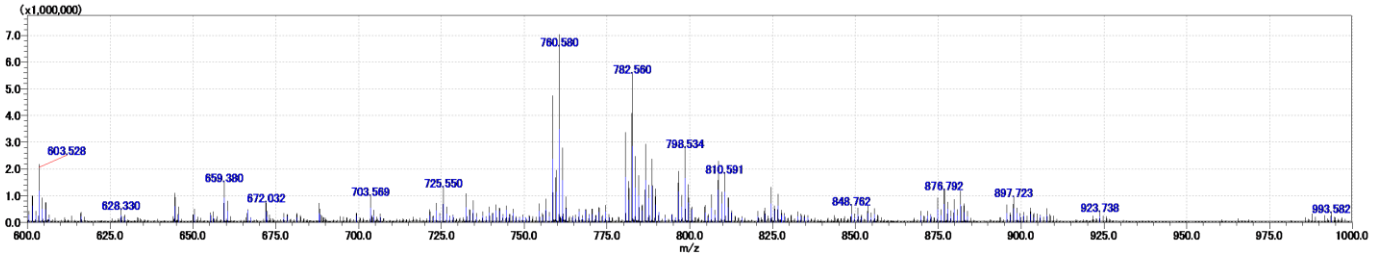
(x1,000,000)
760.580
782.560
603.528
798.534
659.380
810.591
672.032
703.569
725.550
628.330
848.762
876.792
897.723
923.738
993.582
m/z

b)

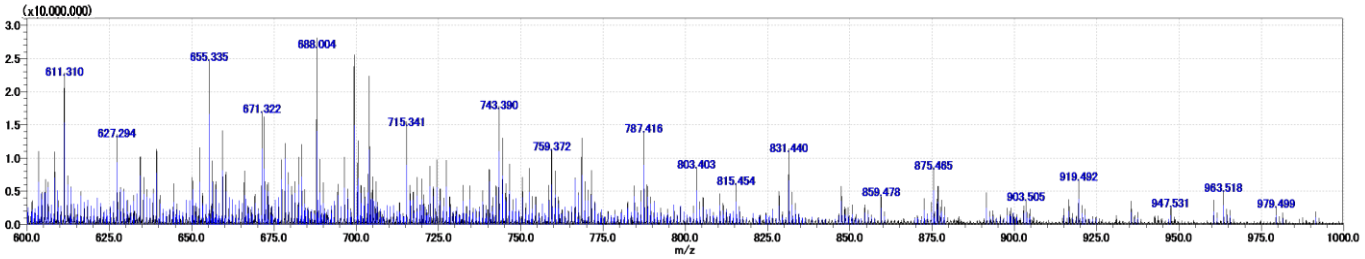
(x10,000,000)
688.004
655.335
611.310
671.322
743.390
715.341
627.294
787.416
759.372
831.440
803.403
875.485
815.454
859.478
919.492
903.505
963.518
947.531
979.499
m/z

Figure 3

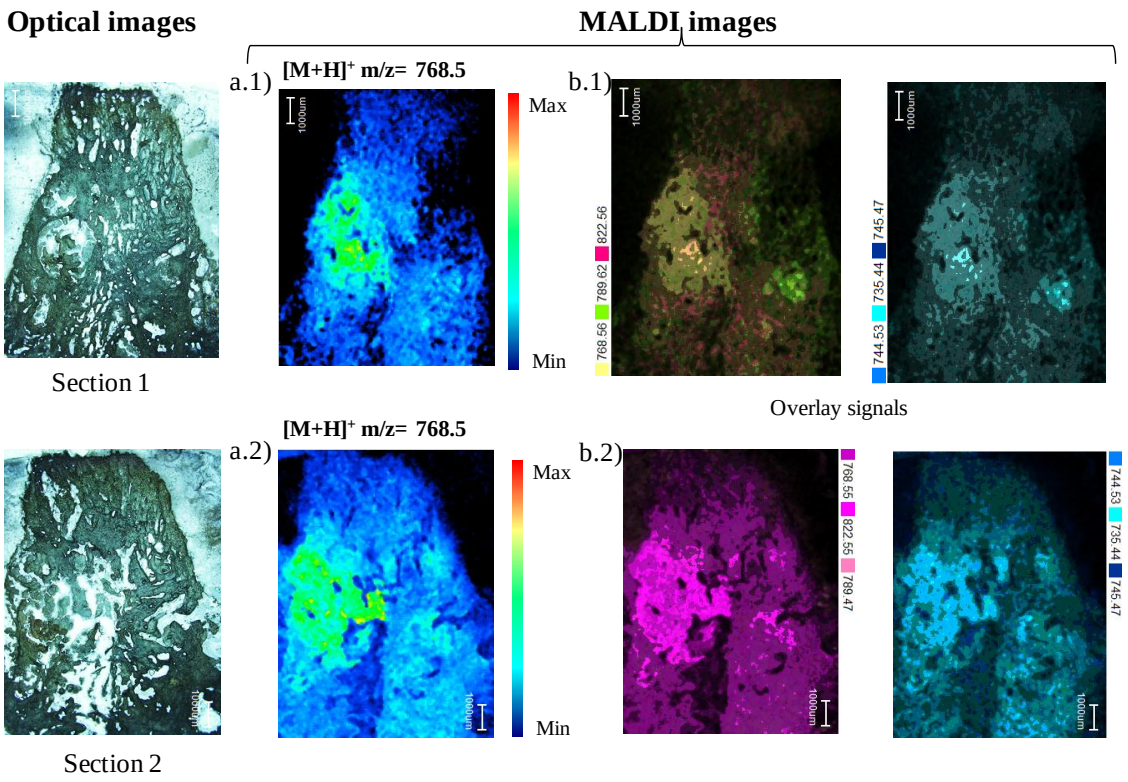
Optical images
MALDI images
a.1)
[M+H]+ m/z= 768.5
Max
Min
b.1)
822.56
789.62
768.56
745.47
735.44
744.53
Section 1
Overlay signals
a.2)
[M+H]+ m/z= 768.5
Max
Min
b.2)
768.56
822.56
789.47
744.53
735.44
745.47
Section 2

Figure 4

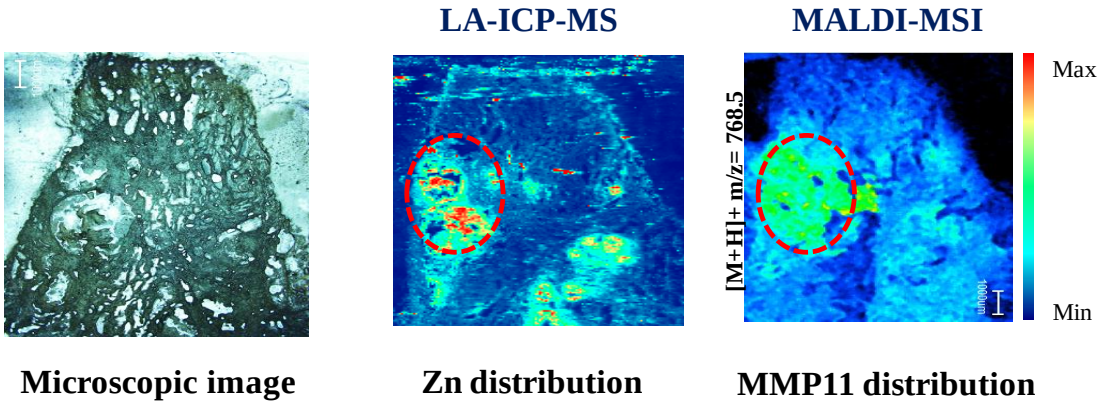
LA-ICP-MS
MALDI-MSI
[M+H]+ m/z= 768.5
Max
Min
Microscopic image
Zn distribution
MMP11 distribution

Table 1 Operating conditions for the ICP-MS and laser ablation systems

Agilent 7500	
RF Power	1500W
Ar make-up gas	0.9 L min^{-1}
Isotopes	^{64}Zn, ^{66}Zn and ^{103}Rh
Adquisiton time	0.1s (^{64}Zn and ^{66}Zn) and 0.05s ^{103}Rh
CETAC LSX-213 laser ablation system	
Laser wavelength	213 nm
Pulse energy	100% (5.6mJ)
Repetition Rate	20 Hz
Spot size	25 µm
Scan speed	100 µm s^{-1}
Carrier gas flow rate	0.8 L min^{-1} He

Table 2 Peptides obtained from the in-situ digested MMP11 and the sequence coverage value from healthy and tumor breast tissue.

***m/z* theoretical**	***m/z* observed (healthy)**	***m/z* observed (tumor)**	**Missed Cleavages**	**Sequence**
605,329	605,298	605,270	0	FDPVK
609,340	609,353	609,294	0	LYWK
639,289	639,353	639,352	0	DYWR
648,310	n.d.	648,183	0	ATDWR
735,394	n.d.	735,285	0	AGFVWR
735,415	735,570	735,432	0	FVLSGGR
744,379	744,403	744,398	0	FHPSTR
745,403	745,433	745,403	0	IYFFR
768,389	768,572	768,528	0	TDLTYR
769,420	769,586	769,458	0	VDSPVRR
789,425	789,445	789,465	0	ALEGFPR
804,411	804,551	804,410	1	RATDWR
822,432	n.d.	822,528	1	GRLYWK
832,493	832,456	832,456	1	FDPVKVK
852,411	852,709	852,491	1	GRDYWR
891,460	n.d.	891,453	0	QTMAEALK
900,480	900,773	900,746	1	FHPSTRR
925,521	925,755	925,753	1	VDSPVPRR
1004,579	1004,597	1004,551	1	AGFVWRLR
1016,589	1016,575	1016,609	1	VKALEGFPR
1051,524	1051,576	1051,570	0	ADIMIDFAR
1150,658	1150,743	1150,739	1	TDLTYRILR
1211,606	1211,688	1211,687	1	WEKTDLTYR
1364,649	1364,790	1364,788	1	DYWRFHPSTR
1450,784	1450,834	1450,832	0	FPVHAALVWGPEK
Coverage %	18	20		

*n.d. = non detected peptides